ACTIVE STRUCTURAL ACOUSTIC CONTROL OF MACHINE ENCLOSURES

Sandor M. Veres and Jian Luo *

* *School of Engineering Sciences,*
University of Southampton
Highfield, SO17 1BJ, Email:sandy@mech.soton.ac.uk m

Abstract: Vibrating machinery such as pumps, generators and compressors normally use passive insulation materials to reduce sound radiation. This paper provides a practical examination of possible solutions to active control of machine enclosures that reduces the radiated sound intensity from the enclosure to the environment. The results show that a combination of simple sky-hook type feedback controllers for active mounts, and relatively straightforward feedforward frequency selective filter (FSF) based controllers for modal control, offer a practical solution.

Keywords: Active vibration control, modal analysis, system identification, adaptive control.

1. INTRODUCTION

Active control of structural vibrations to reduce sound radiation is called active structural acoustic control (ASAC) by Clark and Fuller (1991). Active vibration and sound control has enjoyed tremendous research input in recent years, see for instance Kuo and Morgan (1996); Fuller and von Flotow (1995); Fuller et al.; Tokhi and S. M. Veres (2002).

This paper analyses the problem of, and provides a generic solution to, the active structural acoustic control of an enclosure around noisy machinery (>90dBA). The machine vibration has a broad-band spectrum as shown in Figure 1. The problem is particularly challenging as the combined system dynamics of enclosure/mounting, actuators and of the machine show some nonlinearity. The enclosure itself is fairly linear and allows modal analysis. Because of the large number of modes and complex coupling of the mounts and structural dynamics of the mounts, the idea of complete state-space modelling proved to be impractical, due to modelling inaccuracies and nonlinearities that were affecting the derived controllers to such a degree that controller performance was poor or unstable. There is another reason why complete state space modelling is not practical for state feedback control using an observer: the filtering requirements of the measured outputs, that are needed to cut off high frequency mode vibrations of the enclosure (that appear as disturbances for low frequency mode control), cause detrimental time delays and make a feedback control solution ineffective.

There are several possibilities for feedforward control of complex systems. The filtered X LMS (FXLMS) methods Bjarnason (1995); P. L. Feintuch and Lo (1993) use disturbance source detection signals for feed-forward control. As it is difficult to find well correlated independent ("early detection") signal in this enclosure problem, the novelty of this paper is the adaptation of a frequency selective filter (FSF) Veres (2002) to the enclosure control problem.

The next section outlines the technical problem, then the modelling approaches are presented, the control objectives, optimization of mount locations, suitable controllers for the active mount, the new FSF control scheme is presented with laboratory trials.

2. THE CONTROL PROBLEM

This section describes the machine enclosure used. The main structural elements of the enclosure are its 12mm aluminium plates that are thick enough for bolted assembly of the corners into a six sided L shaped enclosure. This enclosure is intended to be used for a compressor but the laboratory experiments (due to impracticality to run the final compressor in the lab) were using only a mock up machine, that consist of a a steel frame with a powerful AC motor that is geared to several unbalanced shafts and therefore strongly shaking the steel frame at high speed of the motor. There are currently 5 electromagnetic actuators (up to 200N force and bandwidth over 1000 rad/s, these are fitted to active mounts which consist of a spring and a damper.

The enclosure wall is strong enough for the reliable mounting of sensors, electromagnetic and piezo actuators. Fig. 1 shows a photograph of the opened up an experimental enclosure.

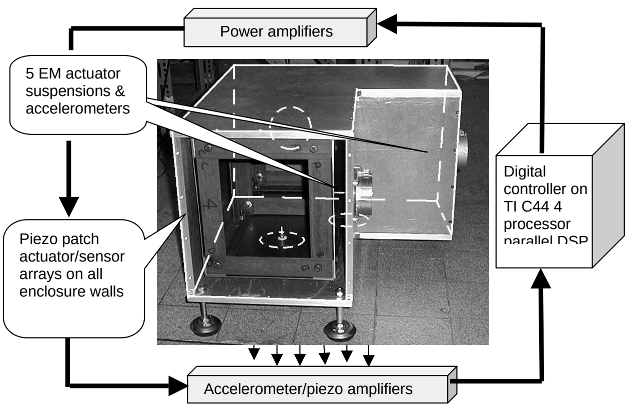

Fig. 1. Enclosure control setup.

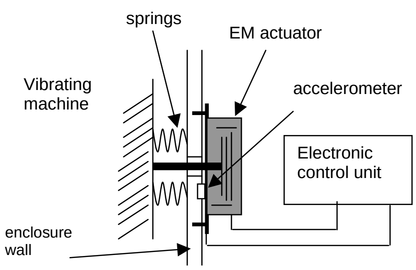

Fig. 2. Electronically controlled suspensions.

3. OVERALL DYNAMICAL MODEL

The machine is vibrating and the spectrum of the vibration near a mount of the enclosure is illustrated in Fig. 3. There are 5 mounting points

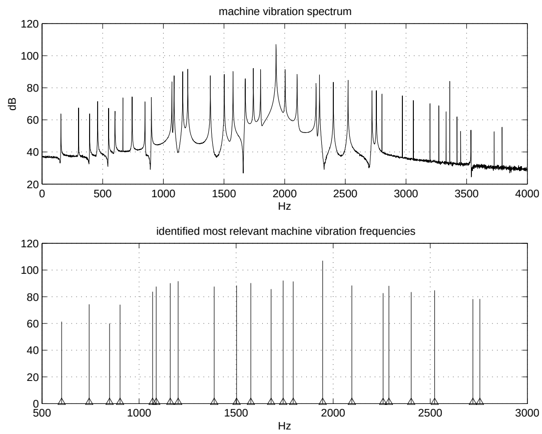

Fig. 3. Machine vibrations at a mount.

of the enclosure to the machine and the enclosure receives excitation from two sources:

(1) Through the spring-damper mounts that can also be controlled by co-located electromagnetic (EM) actuators if these are activated. Without the active control the mounts operate as passive mounts. When control is used the mount will be called an active mount.
(2) Through direct sound radiation from the machine wall via the cavity dynamics between the air filled space between the enclosure and the machine.

Most of the high frequency sound is absorbed by the enclosure wall and the low frequency excitation mostly propagates through the mounts to the enclosure. In this paper the enclosure wall will be controlled to dampen the sound radiation of the enclosure wall due to both of these excitations.

4. ENCLOSURE MODE SHAPES

Mode-shapes will be defined with regard to a two dimensional map that covers the enclosure surface. Thus $\psi_i(x^{(\nu)}, y^{(\nu)}, n)$ denotes the nth mode shape function on side of plate No. ν, where $\nu = 1, 2, ..., 6$ indexes the enclosure plates. Location $[x^{(\nu)}, y^{(\nu)}]$ is understood then in a local coordinate system, fixed once for all. The total surface of the enclosure will be denoted by $\mathtt{S}$. The mode shape function $f_i(x^{(\nu)}, y^{(\nu)}, n)$ means transversal displacements on the surface of the enclosure relative to its vibration free stationary position. Tonal vibration of the enclosure at a single frequency is characterized by

$$w(x, y, \omega)e^{j\omega t} = \sum_n A_n(\omega)\psi_n(x, y, n)e^{j\omega t}$$

where $w(x, y, \omega)$ defines the complex amplitude (hence phase and amplitude) of harmonic transversal motion at a surface point $[x, y] \in \mathtt{S}$ (if it does not cause ambiguity we leave off index ν for simplicity). The complex amplitudes $A_n(\omega)$ are

$$A_n(\omega) = \frac{1}{\omega_n^2 - \omega^2 + 2j\zeta_n\omega_n\omega} \int_{\mathtt{S}} f(x, y, \omega)\psi_n(x, y, n)dxdy$$

where $f(x, y, \omega)$ is an input force distribution.

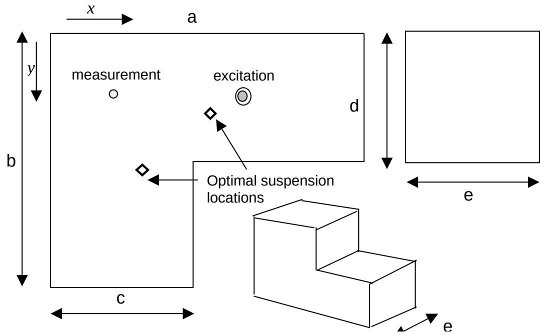

Fig. 4. An excitation point and a measurement point on an L shaped plate of the enclosure.

By linearity the effect of a mix of tones with force distribution described by the Dirac's delta functions δ as

$$f_m(x, y) = \delta_{x_m, y_m}(x, y) \sum_k d_k^m e^{j\omega_k t}$$

at locations $[x_m, y_m] \in \mathtt{S}, m = 1, ..., M$ is described by the time signal

$$W(x, y, t) = \\ = \sum_m \sum_k \sum_n \psi_n(x_m, y_m) \frac{d_k^m e^{j\omega_k t} \psi_n(x, y, n)}{\omega_n^2 - \omega_k^2 + 2j\zeta_n\omega_n\omega_k}$$

A special case of this is when there is only one tone of frequency ω in the input and for a single input location $[x_m, y_m]$ and output measurement point $[x, y]$ this gives transfer function

$$G(\omega; x, y, x_m, y_m) = \\ = \sum_n \psi_n(x_m, y_m) \frac{d_m \psi_n(x, y, n)}{\omega_n^2 - \omega_k^2 + 2j\zeta_n\omega_n\omega_k}$$

An example of a modelled transfer function from the circled point in Fig. 4 to a measurement point is illustrated in Fig. 5, that was obtained by fitting a model using measurements and a structural dynamics software Balmes (1998). From the infinite number of modes here only the most dominant 42 are used in model modelling. The modal model of the enclosure is estimated on the basis of a large number of shaker tests applied to various points on each plate and the measurements were taken by a sliding accelerometer probe that can be held anywhere on the enclosure surface. The most important transfer functions are the ones from piezo disc actuators to piezo disc sensors. Transfer

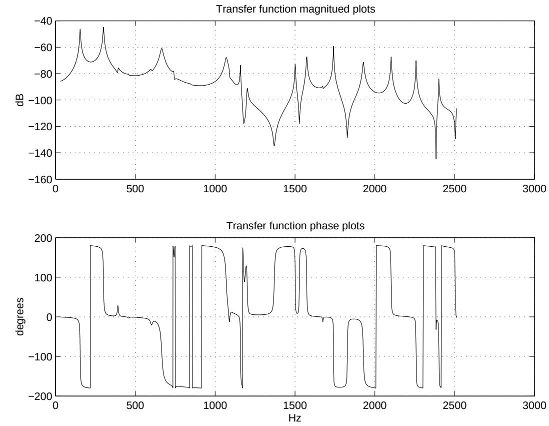

Fig. 5. A transfer function example.

functions from the mounts (without the machine installed) to the piezo discs were also measured to see the transfer from mount locations over the structure. The combined pairwise measurements were processed to obtain the natural frequencies, mode shapes and associated damping ratios by the methods in Balmes (1998). There is no space here to list all the frequencies and damping factors, Fig. 5 illustrates a subset of the relevant frequencies.

5. CONTROL OBJECTIVES

The machine is vibrating and the total power of sound radiation has to minimized. This is proportionate with the volume velocity or rate of volume displacements of the enclosure and is also correlated with the kinetic energy of the enclosure. The total kinetic energy is

$$E = \frac{M}{2S} \int_{\mathtt{S}} (\frac{\partial w(x, y, t)}{\partial t})^2 dxdy$$

For an input spectrum and by the orthogonality of the mode shapes, this can be easily approximated for a given discrete input spectrum at a given set of locations $[x_m, y_m], m = 1, ..., M$:

$$E_{estim} = \frac{M}{4} \sum_n \sum_k v_{nk} v_{nk}^T$$
$$\{v_{nk}\}_m = \frac{d_m \omega_k \psi(x_m, y_m, n)}{\omega_n^2 - \omega_k^2 + 2j\omega_n\omega_k}$$
$$m = 1, 2, ...M$$

In this paper the control objective is to reduce the E by the use of

(1) suitable active mounts and
(2) by feedforward control of the piezo disk actuators on the enclosure surface.

Fig. 6 outlines the overall controller structure used. The active mounts operate independently as no gain was experienced in trials with multivariable control schemes. The mount locations that

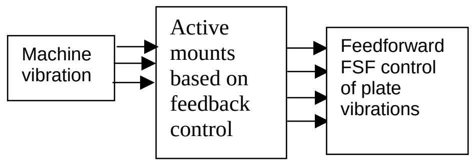

Fig. 6. The controller architecture used.

result in the smallest amount of kinetic energy transfer E_{estim} from the vibration machine to the enclosure are considered the optimal ones. The nonlinear optimization was carried out by the Nelder-Mead simplex methods as in MATLAB. The optimal locations are shown in Fig. 4.

6. ACTIVE CONTROL OF MOUNTS

A block diagram of the a single active mount dynamics is displayed in Fig. 7. The transfer

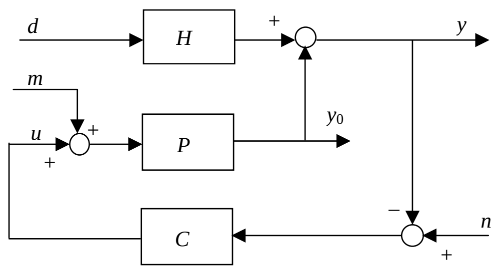

Fig. 7. Block diagram of the active mount feedback system for vibration isolation.

functions involved are

$$H(s) = \frac{fs+K}{ms^2+fs+K}d, \; P(s) = \frac{1}{(ms^2+fs+K)}$$

$$y(s) = P(s)u(s) + H(s)d(s)$$

Here d is the excitation and H is the transfer function of the mount dynamics from the machine vibration to the enclosure mounting through the passive spring damper system. P is the transfer function of the mount dynamics from the electromagnetic actuator to the enclosure mounting point. For passive mounts $C \equiv 0$.

The effective enclosure mass m as seen by one mount is taken as 4kg and the damping coefficients f and spring stiffness K were designed to keep the machine firmly in place without natural vibrations. The softest possible springs have been choosen that still keep the machine in placed Taking 100kp weight of the machine per mounting and permitting it to move 10mm (by pressing in mounting springs), 0.01m $\times$K=100kp gives K=$10^4 kp/m = 10^5 N/m$. This provides a natural frequency of about $\omega_b = \sqrt{K/m} =$ 158rad/s=25Hz. The associated damper coefficient for critical damping is $f = 2m\omega_b =$ $1264 kps/m$. This means that the passive mount has a bandwidth of $f_b = 25$Hz, so for instance at 250Hz the vibration isolation is 23dB which is significant for the high frequency vibrations of the machine. (See dotted line in the top plot of Fig. 8 for the Gain plot of the passive mount.) The

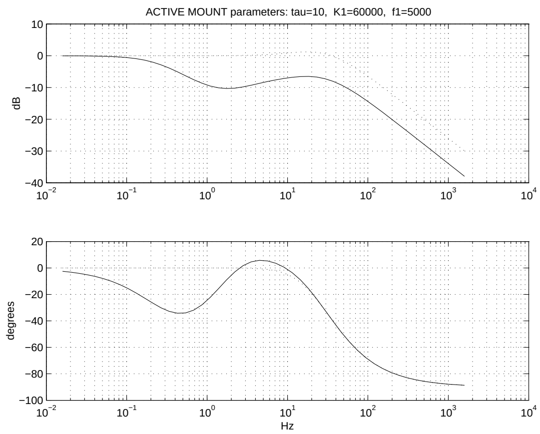

Fig. 8. Bode plots of the vibration isolation dynamics of the passive mount (dashed lines) and the active mount (solid lines).

machine vibrations around and below 25Hz can further be isolated by using the EM actuators to form active mounts using a controller

$$C(s) = \frac{f_1 s - K_1}{(1+s/\tau)^2}$$

This "sky-hook type" of controller contains the square of a first order low pass filter to attenuate high frequency excitation at the mounting accelerometer due to higher mode plate vibration. The top plot in Fig. 9 shows a bandwidth of around 1 rad/s for filtering out high frequency vibrations at the mounting accelerometer.

This simple active mount controller $C(s)$ is easily implemented using analogue circuits (using opamps), hence reducing computational demand for the overall system. Use of analogue circuits for control also avoids inevitable delays associated with digital solutions due to conversion times, sampling cycle and smoothing filters. The active mount performance suffers very little to 20-30% changes in stiffness and damping coefficient values, so a digital system is not needed for adaptation.

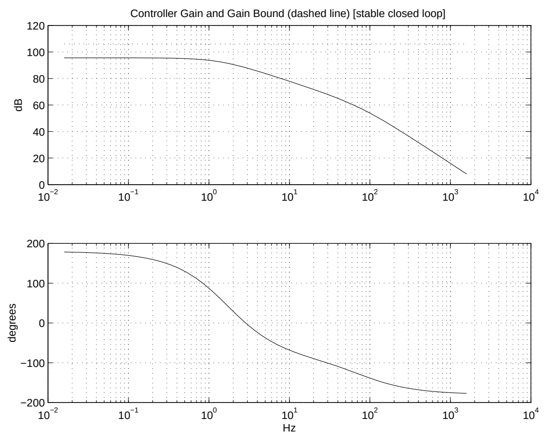

Fig. 9. The controller gain and phase (solid lines) and the gain bound (dashed line) due to actuator limitation.

7. FSF BASED MULTIRATE FEEDBACK/FEEDFORWARD MODAL CONTROL (M2FMC)

FSF based M2FMC can be applied to linear plants where the disturbance spectrum is dominated by a finite set of sinusoidal components, i.e. tonal disturbances. The aim is to iteratively tune a model free controller for the disturbance frequencies and also for modal natural frequencies of the enclosure. For a single frequency the enclosure dynamics can be represented by a complex gain and the signals by complex amplitudes. The complex gain indicates the amplitude and phase shift of a signal passing through a system. Hence the controller can also be implemented by using only two coefficients which reduces the number of necessary calculations to adjust them towards the optimal solution. The method tunes in parallel these complex controller gains for many frequencies (Veres (2002),Meurers et al. (2003)).

Let $\omega_n, n = 1, 2, ..., N$ denote the disturbance and structural natural frequencies of interest.

Let $\mathbf{y}$ denote the measurement signals (S of them) from the piezo array of sensors and use $\mathbf{u}$ (R of them) to denote the array of control signals for the piezo actuators. For a given ω_n the input-output relationship can be described by an equation as

$$\mathbf{y}(\omega_n) = \mathbf{G}(\omega_n)\mathbf{u}(\omega_n) + \mathbf{d}(\omega_n)$$

where

$$\mathbf{y} \stackrel{\text{def}}{=} \begin{bmatrix} y_{r1} \\ y_{i1} \\ \vdots \\ y_{rS} \\ y_{iS} \end{bmatrix} \quad \mathbf{u} \stackrel{\text{def}}{=} \begin{bmatrix} u_{r1} \\ u_{i1} \\ \vdots \\ u_{rR} \\ u_{iR} \end{bmatrix} \quad \mathbf{d} \stackrel{\text{def}}{=} \begin{bmatrix} d_{r1} \\ d_{1i} \\ \vdots \\ d_{rS} \\ d_{iS} \end{bmatrix} \tag{1}$$

$$\mathbf{G} \stackrel{\text{def}}{=} \begin{bmatrix} G_{r11} & -G_{i11} & \cdots & G_{r1R} & -G_{i1R} \\ G_{i11} & G_{r11} & \cdots & G_{i1R} & G_{r1R} \\ \vdots & \vdots & \ddots & \vdots & \vdots \\ G_{rS1} & -G_{iS1} & \cdots & G_{rSR} & -G_{iSR} \\ G_{iS1} & G_{rS1} & \cdots & G_{iSR} & G_{rSR} \end{bmatrix} \tag{2}$$

Here the $\mathbf{y}(\omega_n), \mathbf{G}(\omega_n)$ are obtained by frequency selective filtering (FSF) as described next. $\mathbf{d}(\omega_n)$ is an unknown harmonic signal due to the modal dynamics of the enclosure plates. The objective is to estimate such a $\mathbf{u}(\omega_n)$ that the $\mathbf{y}$ is brought to nearly zero. More precisely, the control criterion will be to minimize the following quadratic cost function

$$J \stackrel{\text{def}}{=} \mathbf{y}^H\mathbf{y} = \sum_{s=1}^{S} |y_s(j\omega_n)|^2 = \sum_{s=1}^{S} \left[(y_{rs})^2 + (y_{is})^2\right] \tag{3}$$

where y_{rs} indicates the real and y_{is} indicates the imaginary part of the s^{th} component of

$\mathbf{y}$. The ^{H} denotes the Hermitian, i.e. complex conjugate, transpose.

The different frequency components of the output signal $\mathbf{y}$ are filtered out by frequency selective filters (FSFs). Iterative tuning of harmonic control for single input single output systems is described for instance in Veres (2002) where convergence properties were proven. Here we adopt it to the multivariable case of the enclosure ASAC problem.

By moving the complex controller gain $\boldsymbol{u}$ into the negative gradient direction of the criterion J the output cost function will be reduced. The gradient of the cost function can be calculated by

$$\nabla\ J = 2\mathbf{G}^T\mathbf{y}. \tag{4}$$

Again it is desired to calculate this gradient without any models for the secondary path transfer function matrix. In the MIMO case it is not enough to perform only one more recording. The number increases to $R \times S$. The following recordings have to be done to calculate the gradient. The first S recordings are to use the conjugate complex output y_s respectively as an addition to input u_1 and use the unchanged remaining $R-1$ inputs. The output vector z_1 is recorded but only the components z_{rs1} and z_{is1} are of interest. The other components can be discarded. The update for the first control signal becomes

$$\begin{bmatrix} u_{r1} \\ u_{i1} \end{bmatrix}_{k+1} = \begin{bmatrix} u_{r1} \\ u_{i1} \end{bmatrix}_k - \mu \sum_{s=0}^{S} \begin{bmatrix} z_{rs1} \\ -z_{is1} \end{bmatrix}_k . \tag{5}$$

This set of recordings is then repeated for every input signal, use the complex conjugate of the previous recorded output signals as an additional input and record the output vector. The controller update for all channels becomes

$$\begin{bmatrix} u_{r1} \\ u_{i1} \\ \vdots \\ u_{rR} \\ u_{iR} \end{bmatrix}_{k+1} = \begin{bmatrix} u_{r1} \\ u_{i1} \\ \vdots \\ u_{rR} \\ u_{iR} \end{bmatrix}_{k} - \mu \sum_{s=0}^{S} \begin{bmatrix} z_{rs1} \\ -z_{is1} \\ \vdots \\ z_{rsR} \\ -z_{isR} \end{bmatrix}_{k} . \quad (6)$$

Next an outline is given to indicate the convergence of the controller gains. The steady state of the given linear stable system can be calculated as

$$\begin{aligned} -[\mathbf{I} - (\mathbf{I} - \mu \mathbf{G}^T \mathbf{G})]^{-1} \mu \mathbf{G}^T (\mathbf{d})_{|q=1} = \\ = - \left(\mathbf{G}^T \mathbf{G}\right)^{-1} \mathbf{G}^T \mathbf{d} \end{aligned} \quad (7)$$

and in the case of the fully-determined system this can be simplified to $(-\mathbf{G}^{-1} d)$.

Therefore the controller converges

(i) for the overdetermined system (S > R) to

$$\lim_{k \to \infty} \mathbf{u}^k = \mathbf{u}_{opt} = - \left(\mathbf{G}^T \mathbf{G}\right)^{-1} \mathbf{G}^T \mathbf{d} \quad (8)$$

(ii) and for the fully-determined system (S=R) to

$$\lim_{k \to \infty} \mathbf{u}^k = \mathbf{u}_{opt} = -\mathbf{G}^{-1} \mathbf{d} \quad (9)$$

where $\mathbf{u} = -\mathbf{G}^{-1}\mathbf{d}$ is the ideal control input to eliminate the noise of the output.

8. EXPERIMENTAL RESULTS

The FSF control system was implemented on a TI C44 quad parallel processor card running compiled C code and the data were analysed in the MATLAB environment. The methodology was so far tested on the control of single L shaped base plate with two active mounts as part of the enclosure while the machine was providing vibration excitation. The kinetic energy of the enclosure's main L-shaped plate was estimated based on E_{est}. As the realtime data are analysed in batches it is possible to serialize the filtering of signals for 66 frequencies. The control signals are synthesized realtime, the iteration steps are done every 0.25s, sampling rate is 32kHz. The method inherently tries to interfere with vibrations in the plate and constantly adapts its gain to achieve that.

The attenuation results are 25% and 45% in terms of the kinetic energies of the main L-shaped plate for the active mount and for joint active mount plus FSF control, respectively.

9. CONCLUSIONS

The multi variable enclosure vibration attenuation problem was given a solution that uses independent active mounts and iterative/adaptive FSF based feed-forward control of plate vibrations that uses multirate sampling and no source detection signal (as filtered-X LMS does, see Bjarnason (1995)).

These solutions appear to be practical and easier to implement than feedback control based on complex state-space models where performance may suffer from changing plant dynamics and from time delays due to output filtering requirements.

REFERENCES

Etienne Balmes. *Structural Dynamics Toolbox (Manual).* Scientific Software, 20 rue Troyon, 92316 Sevres Cedex, Francen, 1998.

E. Bjarnason. Analysis of the filtered-x lms algorithm. *IEEE Trans. Speech and Audio Processing*, 3(3):504–514, 1995.

R. L. Clark and C. R. Fuller. Active Structural Acoustic Control with Adaptive Structures Including Wavenumber Considerations. 1991. In: C. A. Rogers and C. R. Fuller (eds.): Proc. of the 1st Conference on Recent Advances in Active Control of Sound and Vibration. Blacksburg.

C. R. Fuller, S. J. Elliott, and P. A. Nelson. Active Control of Vibration. Academic Press, London etc. 1995.

C. R. Fuller and A. H. von Flotow. Active control of sound and vibration. *IEEE Control Systems Magazine*, 15(6):9–19, 1995.

S. M. Kuo and D. R. Morgan. *Active Noise Control Systems.* John Wiley and Sons, New York, 1996.

T. Meurers, S. M. Veres, and A.C.H. Tan. Model-free frequency domain iterative active sound and vibration control. *Control Engineering Practice*, 11(2003):1049–1059, 2003.

N. J. Bershad P. L. Feintuch and A. K. Lo. A frequency domain model for filtered lms algorithm - stability analysis, design, and elimination of the training mode,. *IEEE Trans. Acoust. Speech, and Signal Processing*, ASSP-41:1518–1531, 1993.

M. O. Tokhi and Eds. S. M. Veres. *Active sound and vibration control.* IEE, ISBN 0 85296 038 7, Stevenage, London, 2002.

S. M. Veres. Adaptive harmonic control. *Int. J. Control*, 2002.